

Effect of Fire Source Shape and its Size in a Tunnel Fire

Yasushi Oka¹, Hitoshi Kurioka², Hiroomi Satoh²,
Atsumi Miyake¹ and Terushige Ogawa¹

¹ *Department of Safety Engineering, Yokohama National University
79-5 Tokiwadai, Hodogaya-ku, Yokohama, Kanagawa 240-8501*

² *Kajima Technical Research Institute, 19-1 Tobitakyu 2 Chome, Chofu-shi, Tokyo 182-0036*

Abstract

Experiments were carried out to investigate the effects of fire source shapes and those sizes to the fire property using the model tunnel which has a rectangular cross section and its aspect ratio is 1:2. Square and rectangular burners were used as model fire sources. Heat release rate was changed from 4.5 to 36 kW in proportional to the fire size and longitudinal ventilation velocity also varied in the range of 0 to 0.8 m/s. Flame tilt angle, maximum temperature rise of smoke layer near the ceiling and its position were adopted as the variables which characterise the fire phenomena in the near field of fire source in the presence of longitudinal ventilation. New empirical formulae considering the effects of the fire source shapes and those sizes for these variables were developed.

1. Introduction*

Tunnels for vehicles and railways are a part of the important infrastructure which supports our comfortable life and becomes a main artery which plays an important role for transport of goods and human. However, latent hazards have increased with the enlargement of the volume of traffic and loading combustibles which pass through the tunnel and/or with the demand to cut transport time (high-speed running) for these 20 years.

Many papers on tunnel fires focused on the smoke control with longitudinal ventilation system [1-6]. In order to predict the extent of high temperature region including flame propagation and to estimate the damage to the tunnel structure, it is important to investigate the radiation intensity in the near field of the fire source from the point of view of fire prevention. However, few papers have tackled on representing the flame behaviour and fire property in the near field of the fire source affected by forced longitudinal ventilation in tunnel.

Corresponding Author- Tel.: +81-45-339-3921;

Fax: +81-45-339-4011

E-mail address: y-oka@ynu.ac.jp

Kurioka et al [7] have conducted a series of experiments using model tunnels, having a rectangular cross section with several aspect

ratios, to make a flowchart for evaluating the extent of damage region of tunnel structure caused by unwanted fire in design stage. They reported the empirical formulae to predict and describe not only the flame tilt angle but also the maximum temperature of smoke layer and its location in the presence of longitudinal ventilation. However, the effects of the size and shape of fire source are not incorporated in these empirical formulae, since a unique square fire source was employed in their experiments. However, it is considered that the size and shape of fire source becomes one of the key parameter to control the fire property in tunnel as well as fire intensity, ventilation condition, cross-sectional shape of tunnel and position of fire source, because the accidents related to the single tank lorry which loads with combustible materials and accidents involved multi vehicles in traffic congestion, etc. are reported in the automobile tunnel.

The objective of the current work is firstly to make clear experimentally the effects of size and shape of fire source on flame tilt angle and temperature of smoke layer, in secondary to examine the application range of the existing empirical formulae [8] and finally to develop alternate empirical formulae considering the factor related to the fire source geometry, provided that the application range is limited.

2. Experimental Procedure

2.1 Outline of model tunnel

Figure 1 shows a schematic diagram of the experimental apparatus. The major part of model tunnel was made of steel plate with a

thickness of 2 mm, with the ceiling lined 10 mm thick fireproof blanket to the distance of 0.45 m in both directions from the fire source. The side wall was also made of fireproof glass to observe the flame shape. This model tunnel has a rectangular cross section of 0.6m (width) x 0.3m (height) and is 5.4m length. To simulate a longitudinal ventilation system, we installed a mechanical fan with inverter control at the air supply inlet and fresh air was pushed into the model tunnel through a fine mesh filter zone to stabilize the flow distribution. The downstream openings was fully open for unrestricted air flow.

2.2 Experimental condition

As shown the experimental condition in Table 1, we totally conducted 123 tests with changing size of square fire source, aspect ratio defined by length and width of rectangular fire source and the direction of rectangular fire source facing the longitudinal ventilation velocity. Heat release rate was varied in the range of 4.5 to 36 kW. These are calculated values assuming complete combustion based on the amount of LPG. The longitudinal ventilation velocity was varied in the range of 0 to 0.8 m/sec. These are predefined values which are calculated based on the relationship between the output of hot wire anemometer installed in air supply zone and a representative mean longitudinal ventilation velocity passing above the fire source without flame. This representative mean longitudinal velocity, by dividing the measured total volumetric flow by the effective cross-sectional area of model tunnel, was employed for the analysis.

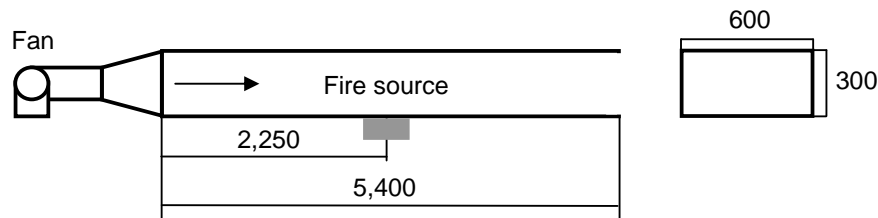


Figure 1 Schematic diagram of model tunnel. unit:mm

Experimental project was composed of three series with the variation of the fire source shape. In A series tests, square porous burners of three kinds of size were used. In B series tests, rectangular porous burners of three kinds of size were used and set the long side of rectangular burner facing the longitudinal ventilation. In C series tests, three kinds of same rectangular burners employed in B series were used and set the short side of rectangular burner facing the longitudinal ventilation. According to the problems for the capacity of air supply fan and for the heat-resistance of model tunnel, it was impossible to make the value of Q^* in A3 series to be a same value in A1 and A2 series. The heat release rates for A1, A2, B and C series were almost same and were set ranging from 0.2 to 4.5 for Q^* and/or Q^*_{rec} .

Model fire source

Square and rectangular fire sources were employed. The former was used in A series tests and latter was used in B and C series test. The centre of each porous gas burner was positioned 2.25 m from the air supply inlet and aligned with the tunnel axis, even if burner shape and size was changed. Liquefied propane gas was used as a fuel. The surface of the fire source was flush with the tunnel floor.

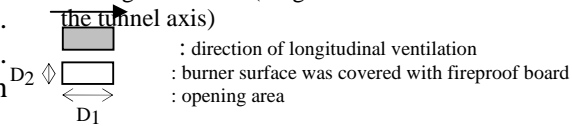
Temperature measurement

The temperature field generated by the tilted flame and plume was measured using K-type thermocouples with a diameter of 0.65 mm. Thermocouples were arranged to cover a downstream region of 0.725m(W) x 0.29m(H) along the tunnel axis with the datum set at the centre of the burner. Temperature of smoke layer was also measured using same thermocouples installed along the tunnel axis at 10 mm below the ceiling. Maximum temperature of smoke layer and its position was decided using these data.

Table 1 List of the experimental condition

series	HRR (kW)	Ventilation Velocity (m/s)	Note
A	A1 4.5 9 12	0, 0.2, 0.3, 0.5, 0.8 0, 0.2, 0.3, 0.5, 0.8 0, 0.3, 0.5, 0.8	0.1m x 0.1m → □
	A2 4.5 9 24	0, 0.2, 0.3, 0.5 0, 0.3, 0.5, 0.8 0.3, 0.5, 0.8	0.2m x 0.2m → □
	A3 4.5 9 36	0, 0.2, 0.3, 0.5 0, 0.3, 0.5, 0.8 0.2, 0.3, 0.5, 0.8	0.3m x 0.3m → □
B	B1 4.5 9 12 24	0, 0.2, 0.3, 0.5 0, 0.3, 0.5, 0.8 0, 0.2, 0.3, 0.5, 0.8 0, 0.2, 0.3, 0.5, 0.8	0.2m x 0.1m → ▨
	B2 4.5 9 18 24	0, 0.2, 0.3, 0.5 0, 0.3, 0.5, 0.8 0, 0.2, 0.3, 0.5, 0.8 0.3, 0.5, 0.8	0.3m x 0.1m → ▨
	B3 9	0, 0.3, 0.5, 0.8	0.3m x 0.15m → ▨
C	C1 4.5 6 9 12 24	0, 0.2, 0.3, 0.5, 0.8 0.8 0, 0.3, 0.5, 0.8 0, 0.2, 0.3, 0.5, 0.8 0, 0.2, 0.3, 0.5, 0.8	0.1m x 0.2m → ▨
	C2 4.5 6 9 18 36	0, 0.2, 0.3, 0.5, 0.8 0.3, 0.5, 0.8 0 0, 0.2, 0.3, 0.5, 0.8 0	0.1m x 0.3m → ▨
	C3 9	0, 0.3, 0.5, 0.8	0.15m x 0.3m → ▨

A: square burner, B: rectangular burner (long side of burner was set perpendicular to the tunnel axis), C: rectangular burner (long side of burner was set along the tunnel axis)



Isotherms were constructed using these measured temperatures to find the tilt angle of flame and/or hot current axis. Depending on the heat release rate and the magnitude of the longitudinal ventilation, the flame tip sometimes extended beyond the net of thermocouples to make it impossible to delineate the flaming region. Reported temperatures are taken as an average over the last 3 minutes of a 10 minutes test and include the effect of radiation from flame and warmed boundaries. This duration was chosen to achieve at a quasi steady state for

both heat release rate and longitudinal ventilation velocity. The data were logged in every 5 seconds on a PC.

Definition of other variables

The situation whether flame touching to the tunnel ceiling or not was varied depending on the conditions such as heat release rate, longitudinal ventilation velocity and tunnel height. Moreover, the upward velocity close to the fire source has relatively weak buoyancy compared to the potential of longitudinal ventilation and the flame is pushed downstream, showing a spread at the base of the flame. The upward velocity, however, gradually increases as buoyancy increases with height and flames tend to rise vertically. The locus of trajectory of flame and/or hot current is shown in Figure 2 by dashed line. According to the definition described in previous report [8], the axis of flame and/or hot current is pushed downstream at distance X_1 from the centre of the burner surface and rises at the angle θ and impinges on the tunnel ceiling. Flame and/or hot current, which impinges on the tunnel ceiling, propagates in upstream and downstream directions from the impinged position, but only the propagation downstream is considered in this paper.

3. Results and Discussions

3.1 Comparison between measured data and reported empirical formulae

Maximum temperature rise of smoke layer

The results of the maximum temperature rise of smoke layer in the presence of longitudinal ventilation using the variables represented in the literature[8] are shown in Figure 3. As the data of A1 which employed a square porous burner of 0.1 m x 0.1 m are matched closely the predicted value which is described in solid line, the reproducibility of this experiment can be confirmed.

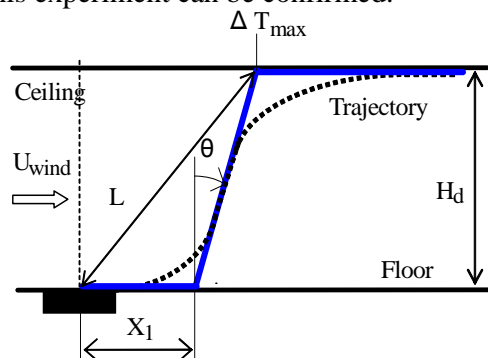


Fig. 2. Definition of variables.

Dotted and solid lines mean real and modelled trajectory, respectively.

The maximum temperature of the smoke layer tends to gradually become lower with the increase of fire source area, even if the similar square fire source was employed in A2 and A3 tests. However it is confirmed that the dependency of the maximum temperature rise of smoke layer for the combined function of Q^* and Fr shows the same tendency irrespective of the difference of the fire source area.

It was observed in A3 tests that flame showed not luminous but pale blue in the upstream side of the burner at the low heat release rate of 4.5 kW. However, in the case of flames touching directly to the tunnel ceiling under the condition of the heat release rate being 24kW(A2), 36kW(A3), maximum temperature rise coincides with upper limit of predicted values. The results

in B series tests are shown in Figure 3(b). It is confirmed that maximum temperature rise was sensitive to the length of rectangular burner facing the longitudinal ventilation velocity and showed lower value according to the length being longer from B1 to B2 than predicted value. In C series tests, the results at the condition of small heat release rate as $Q=4.5$ kW and 6kW and large ventilation velocity as 0.8m/s, which are symbolized in “*” became much lower maximum temperature rise than predicted values and showed different dependency for the combined function of Q^* and Fr . It was considered that the fire plume did not impinge on the tunnel ceiling because of the maximum temperature rise of smoke layer being less than 130K. Other results except for these 4 cases were scattered on the predicted line irrespective of the aspect ratio of rectangular burner.

Maximum temperature position and flame

tilt angle

As described in the literature[8], maximum temperature position can be arranged in each

and experimental results on maximum temperature of smoke layer.

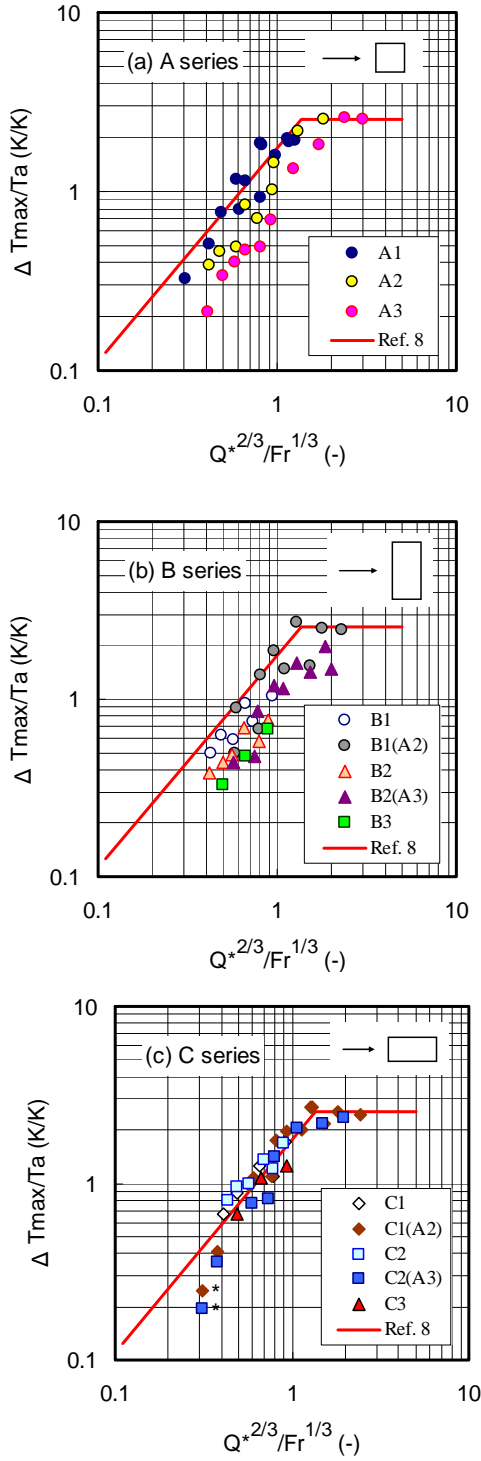


Figure 3 Comparison between predictive values

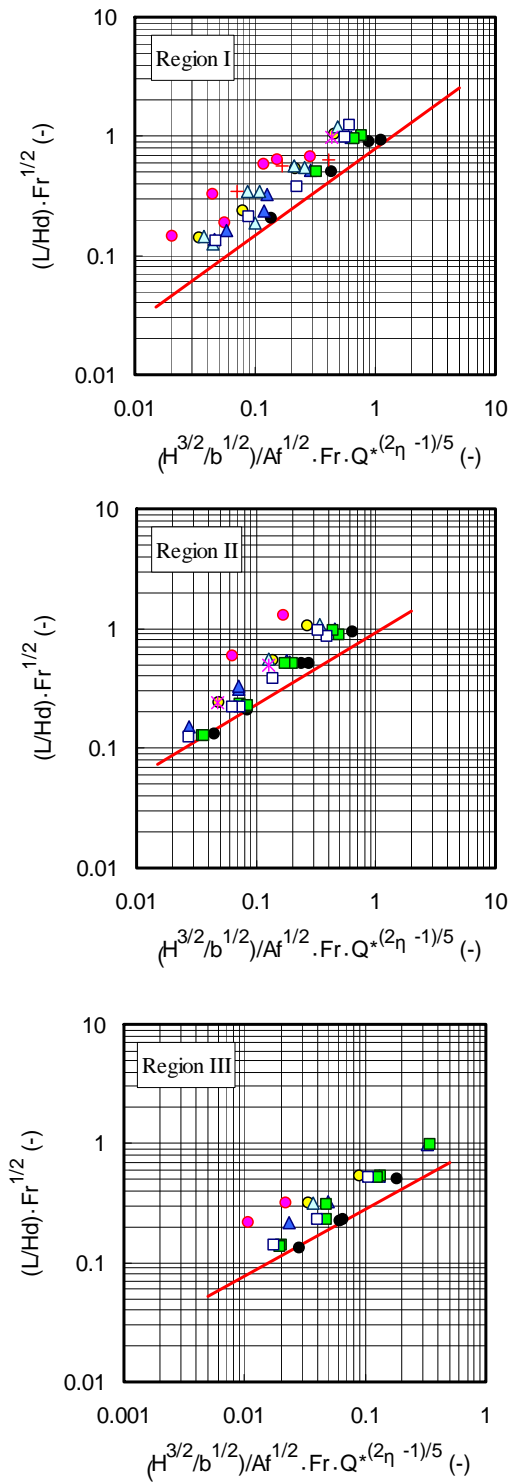


Figure 4 Comparison between predictive

values and experimental results on maximum temperature position

region which was judged based on the maximum temperature rise of smoke layer. This region corresponds to the relative positional relation between flame and tunnel ceiling and would be explained as follows.

Region I : corresponds to the situation in which the flame does not impinge on the tunnel ceiling.

Region II : corresponds the middle region of Region I and III.

Region III: corresponds to the situation in which the flame completely impinges on the tunnel ceiling and extends to downstream along the tunnel ceiling.

Therefore, the experimental results obtained in this study were also arranged with the similar technique. Typical results of maximum temperature position and flame tilt angle were shown in Figure 4 and 5, respectively. The following matters can be read from these figures.

Characteristics of A series

A1 test results on both maximum temperature position and flame tilt angle almost coincided with the predictive values. As well as the results of the maximum temperature rise of smoke layer for A2 and

A3 tests, the maximum temperature position appeared at further downstream side than predicted value and flames fell down with the increase of the fire source area being large. It was considered that the value of Q^* gradually decreases with the increase of fire source area and flames receive the effect of the ventilation as the fire source length facing the longitudinal ventilation becomes large.

Characteristics of B series

The maximum temperature appeared in further downstream position and the flame tilt angle showed larger value than predicted values. Though it is not remarkable like A

series results, the maximum temperature position appeared in the downstream side, according as the aspect ratio of rectangular fire source increases from B1 to B2. Similarly, flame tends to have a large tilt angle, as the long side length of rectangular fire source becomes larger.

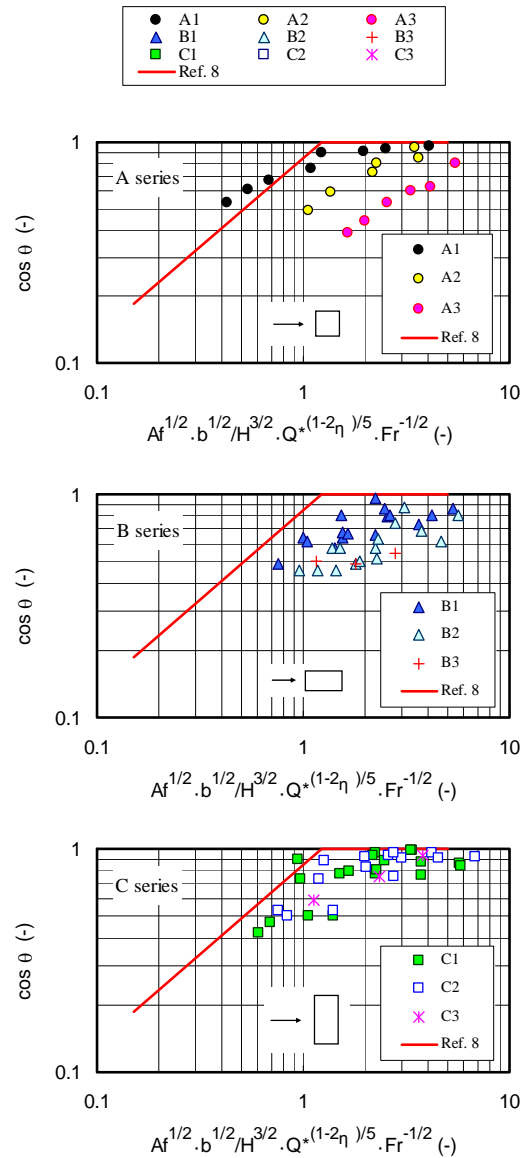


Figure 5 Comparison between predictive value and experimental results on flame tilt angle.

Characteristics of C series

Although the length facing the longitudinal ventilation is equal among A1, C1 and C2, the results of C1 and C2 on maximum temperature position and flame tilt angle does not correspond to that of A1. C1 and C2 tests were also conducted under the almost same condition for both heat release rate and ventilation velocity. If fire plumes in both C1 and C2 tests rise with same inclination angle from the edge of downstream side of the fire source and impinge on the tunnel ceiling, the value of “L” should increase according to the length of rectangular burner becoming longer. Because the starting point of fire plume is moved to downstream side and the length “L” is defined as the distance connecting by the straight line from the maximum temperature position to the centre of fire source. It is then considered that the maximum temperature position appeared in further downstream position than that in A1 test. However, the results on both C1 and C2 tests showed almost same length. This means that the tilt angle of fire plume varied depending on the burner shape. Large amount of fuel was supplied to C2 burner than C1 burner, even if the value of Q^*_{rec} is equal. In this experiment, LPG was employed as the fuel and unburned fuel above the rectangular burner was pushed downstream by the longitudinal ventilation and accumulated at around the downstream edge of the rectangular burner. Therefore, the uniform combustion reaction does not proceed over the rectangular burner surface in actually, the locally active combustion is accelerated at around the downstream edge of the rectangular burner. The force in C2 tests which controls flame inclination to the downstream side worked larger than that in C1.

Applicability of existing empirical formulae

The results except of A1 series do not coincide with predicted values. It is required to develop the alternative method for considering the effect of fire source shape and size. As the dependency to the combined function was hold, it is suggested that all data can be arranged in same manner by incorporating the new variable for representing the effect of fire source shape and size into the existing combined function.

3.2 Suggestion of new variable for accounting the effect of fire source size and shape

New dimensionless variable

We paid attention to the fire plume spread to the tunnel wall along the tunnel axis under the condition that the moderate longitudinal forced ventilation is operating. The flow behaviour of fire plume is considered as follows. The upward velocity close to the fire source has relatively weak buoyancy compared to the potential of longitudinal ventilation and the flame is pushed downstream, showing the spread at the base of the flame. The upward velocity, however, gradually increases as buoyancy increases with height and the fire plume tends to rise vertically with spreading its width from the fire source width, D_2 . And the fire plume impinges on the tunnel ceiling and finally spreads in whole tunnel width, b . It is considered that the ratio between fire source width and tunnel width affects the fire plume behaviour. We employed the dimensionless length, (b/D_2) as a key parameter for representing the effect of fire source size and shape. The dependency of this new parameter to the existing combined function is uncertain. We therefore assumed that this new term would contribute in n -th power and incorporated it into existing empirical formulae.

Decision of value of power n

The variation of the correlation coefficient

against the value of the power of (b/D_2) was examined, after new dimensionless length, (b/D_2) , is substituted into the relation between maximum temperature of smoke layer and combined function. The value of

$$\alpha_1=0.60 \quad \beta_1=6/5$$

$$3.3 \leq (Q^{*2/3}/Fr^{1/3})(b/D_2)^{1/2} < 8$$

$$\alpha_1=2.53 \quad \beta_1=0$$

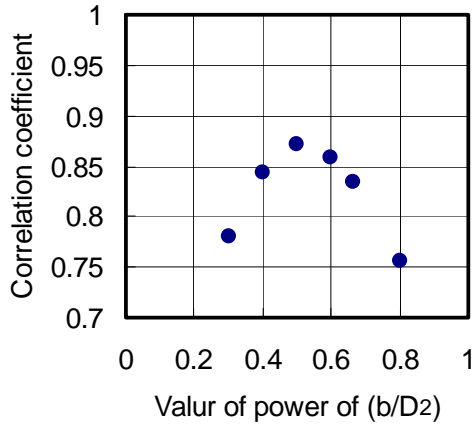


Figure 6 Variation of correlation coefficient against the value of power of (b/D_2) .

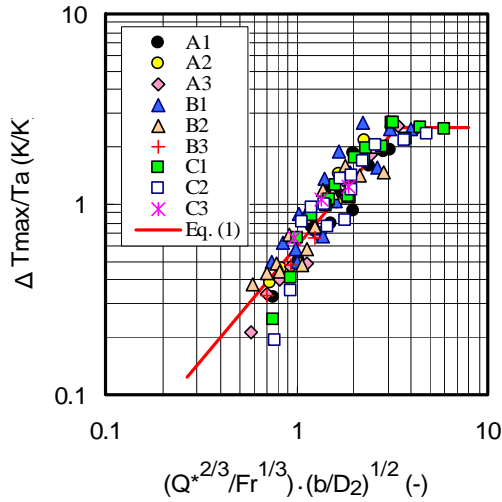


Figure 7 Variation of maximum temperature of smoke layer under the tunnel ceiling against the new combined function of Q^* , Fr and (b/D_2)

$$\frac{\Delta T_{\max}}{T_a} = \alpha_1 \left(\frac{Q^{*2/3}}{Fr^{1/3}} \cdot \left(\frac{b}{D_2} \right)^{1/2} \right)^{\beta_1} \quad (1)$$

$$(Q^{*2/3}/Fr^{1/3})(b/D_2)^{1/2} < 3.3$$

$n=1/2$ showed the maximum value as shown in Figure 6. This dimensionless length was also incorporated into equation which represents the relation between maximum temperature rise position and combined function. Similarly, the correlation coefficient showed the highest value when $n=1/2$, regardless of the region I, II and III. The values of correlation coefficient for region I, II and III were 0.9048, 0.9275 and 0.9188, respectively. We decided to adopt $n=1/2$ for the value of the power of (b/D_2) .

Maximum temperature of smoke layer

All data of maximum temperature rise are plotted with the aid of the new function as shown in Figure 7. In comparison with Figure 3, it can be confirmed that the dispersion of each experimental result becomes small by introducing the new dimensionless length.

The data can be matched closely by the following expression, equation (1).

Maximum temperature position

The results of arranging the maximum temperature position in every region are shown in Figure 8. It can be confirmed that the dispersion becomes small by incorporating $(b/D_2)^{1/2}$ term into the y-axis. The values of power and coefficient were decided with the aid of the experimental results in each region. Final formula for maximum temperature position is given in equation (2). The value of η is decided in every region, which is judged based on the value of ΔT_{\max} .

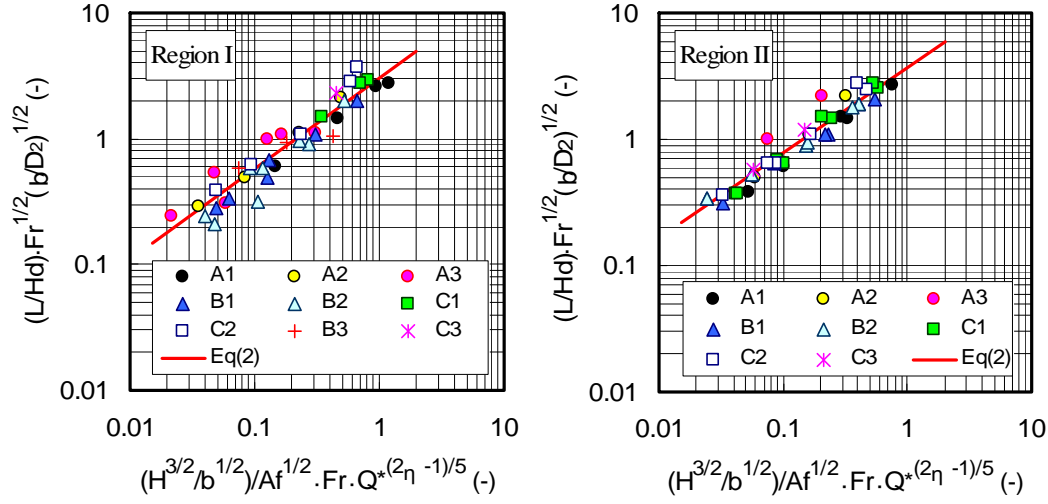
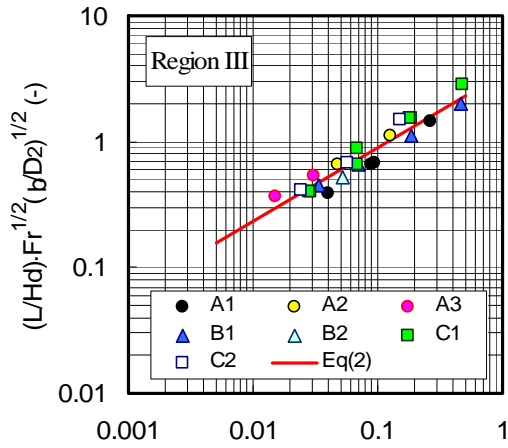


Figure 8 Relation between maximum temperature position and new combined variable.

Region I : $\Delta T_{\max} < 250$ K

Region II : $250 \text{ K} \leq \Delta T_{\max} < 550$ K

Region III : $550 \text{ K} \leq \Delta T_{\max}$



$$\frac{L}{H_d} \cdot Fr^{1/2} \cdot \left(\frac{b}{D_2}\right)^{1/2} = \alpha_2 \left[\frac{H^{3/2}/b^{1/2}}{A_f^{1/2}} \cdot Fr \cdot Q^{*(2\eta-1)/5} \right]^{\beta_2} \quad (2)$$

	η	α_2	β_2	ΔT_{\max}
Region I	-1/3	3.0	0.71	<250 K
Region II	0	3.7	0.67	250 - 550 K
Region III	1/2	3.5	0.59	≥ 550 K

Flame tilt angle

As the results of flame tilt angle showed different property, we thought that the flame

tilt also has peculiar property depending on the situation that flame impinges on the tunnel ceiling as well as maximum temperature positions. Flame tilt data were therefore classified into three regions depending on the maximum temperature rise and they were arranged in the every region and shown in Figure 9.

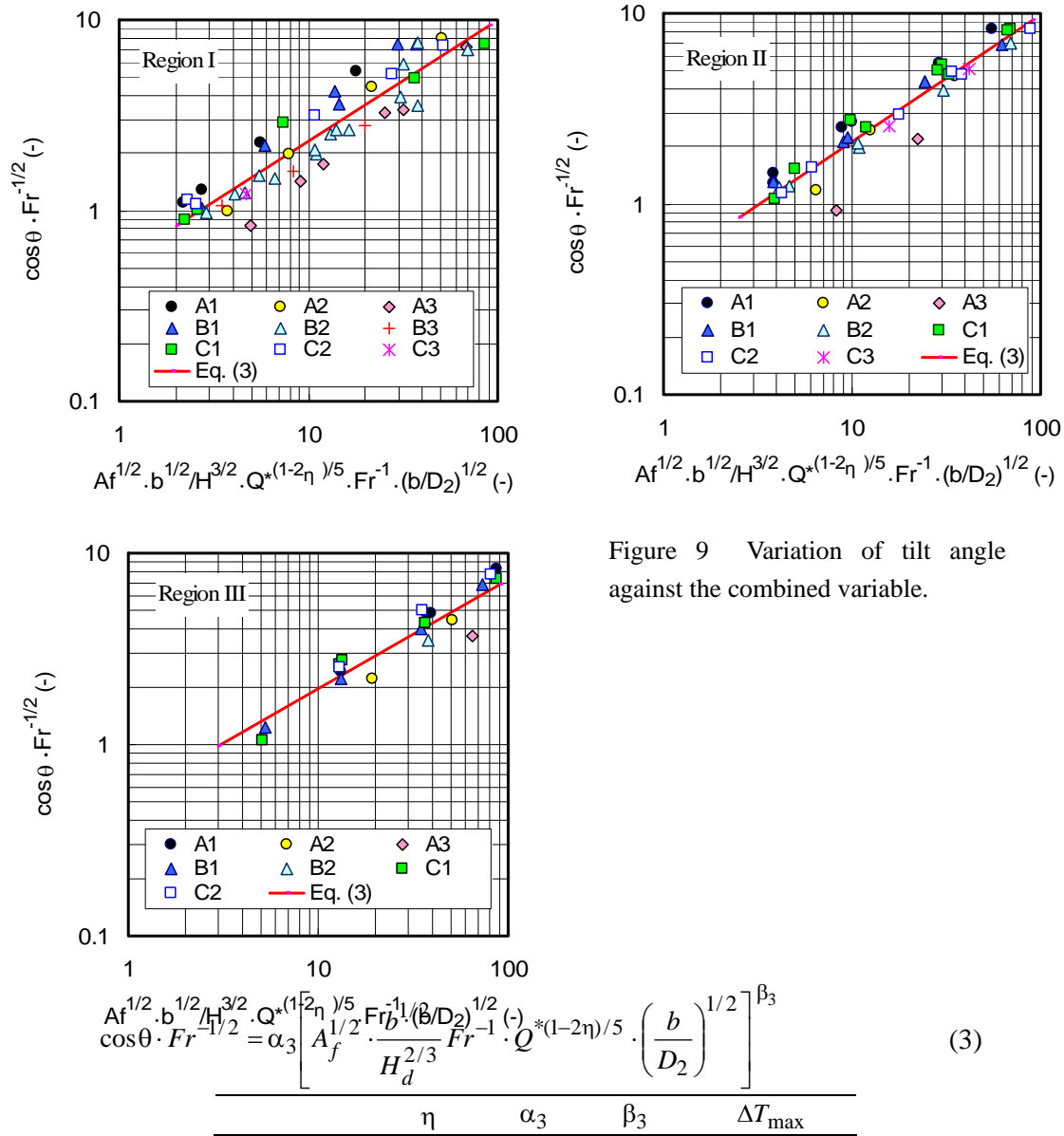


Figure 9 Variation of tilt angle against the combined variable.

Region I	-1/3	0.54	0.63	<250 K
Region II	0	0.46	0.66	250 - 550 K
Region III	1/2	0.52	0.57	≥ 550 K

There is the general improvement compared to the previous arrangement method. However, flame in A3 test showed large tilt angle in comparison with other data irrespective of the region. The cause seems to arise from the difference for the value of Q^* , especially the value of Q^* in A3 test is small than that of other experiments. However, it can be described by arranging in each region and be expressed in equation (3).

4. Conclusions

A series of tests were conducted to investigate the effect of fire source size and shape to the fire properties in the near field of the fire source and following conclusions came across.

- 1) The size and shape of fire source affects the fire properties, as example flame tilt angle, maximum temperature rise of smoke layer and its position, in the presence of longitudinal ventilation.
- 2) Employing dimensionless length, $(b/D_2)^{1/2}$, defined by tunnel width and fire source length facing the longitudinal forced ventilation, the effect of the fire source size and shape can be taken into account and new empirical formulae are developed by incorporating this dimensionless length.

References

- 1) Thomas, P.H., "The movement of smoke in horizontal passages against an air flow", Fire Research Note 723, 1968.
- 2) Oka, Y. and Atkinson, G.T., "Control of Smoke Flow in Tunnel Fires", Fire Safety Journal, Vol.25, pp.305-322, 1995.
- 3) Atkinson, G.T., and Wu, Y., "Smoke control in sloping tunnels", Fire Safety

Journal, Vol.27, pp.335-341, 1996.

- 4) Grant, G.B., Jagger, S.F. and Lea, C.J., "Fires in Tunnels", Phil. Trans. R. Soc. Lond A, Vol.256, pp.2873-2906, 1998.
- 5) Wu, Y. and Bakar, M.Z.A., "Control of smoke flow in tunnel fires using longitudinal ventilation systems – a study of the critical velocity", Fire Safety Journal, Vol.35, pp.363-390, 2000.
- 6) Kunsch, J.P., "Simple model for control of fire gases in a ventilated tunnel", Fire Safety Journal, vol.37, pp.67-81, 2002.
- 7) Kurioka, H., Oka, Y., Satoh, H., Kuwana, H. and Sugawa, O., "Properties of Plume and Near Fire Source in Horizontally Long and Narrow Spaces", Journal of Constr. Engng, AIJ, No.546, pp.151-156, 2001, in Japanese
- 8) Kurioka, H., Oka, Y., Satoh, H., and Sugawa, O.: "Fire Properties in Near Field of Fire Source with Longitudinal Ventilation in Tunnels", Fire Safety Journal, Vol.38, No.4, pp.319-340, June 2003.

Nomenclature

- A_s : cross sectional area of model tunnel [m^2]
 A_f : area of fire source ($D_1 \times D_2$) [m^2]
 b : model tunnel width [m]
 C_p : specific heat at constant pressure [$kJ \cdot kg^{-1} \cdot K^{-1}$]
 D_1 : long side length of fire source [m],
 D_2 : short side length of fire source [m]
 g : acceleration due to gravity [m/sec^2]
 H_d : height from the surface of fire source to tunnel ceiling [m]
 L : distance from the position that flame and/or hot current axis impinged on the tunnel ceiling to the centre of fire source (m)
 Q : heat release rate (kW)
 T_a : temperature of ventilation air (K)

T_f : representative temperature in each region of the fire plume (K)

ΔT : excess temperature (K)

ΔT_{\max} : maximum excess temperature of smoke layer at downstream region (K)

U_{wind} : representative longitudinal ventilation velocity (m/s)

X_1 : horizontal length from the intersection created by the extrapolated plume axis to the centre of the burner surface (m)

$\alpha, \beta, \gamma, \varepsilon$: experimental constants

η : coefficient determined in each region

$\eta = -1/3$ (Region I), $\eta = 0$ (Region II),

$\eta = 1/2$ (Region III)

ρ_a : density of ventilation air ($\text{kg} \cdot \text{m}^{-3}$)

θ : angle created by the intersection of the floor level and extrapolated plume axis (degree)

$$\text{Fr} = U_{\text{wind}}^2 / (g \cdot H_d) \quad [-]$$

$$Q^* = Q / (\rho_a C_p T_a g^{1/2} H_d^{5/2}) \quad [-]$$

$$Q_{\text{rec}}^* = Q / (\rho_a C_p T_a g^{1/2} D_1 D_2^{3/2}) \quad [-]$$

Acknowledgments

The authors would like to thank Mr. Yoshiaki Arai of Kajima Technical Research Institute, Miss. Kozue Hagiwara and Miss Hiroko Yokota of Musashi Institute Technology for help in carrying out the experiments.